**Journal of Plankton Research** Vol.22 no.10 pp.1945–1960, 2000

# Seasonal variations of size-fractionated phytoplankton along the salinity gradient in the York River estuary, Virginia (USA)

Yongsik Sin[1], Richard L.Wetzel and Iris C.Anderson

*College of William and Mary, Virginia Institute of Marine Science, School of Marine Science, Gloucester Point, Virginia 23062, USA*

*[1]Present address: United States Environmental Protection Agency, 2111 S.E. Marine Science Drive, Newport, Oregon 97365, USA*

**Abstract.** The dynamics of phytoplankton size structure were investigated in the freshwater, transitional and estuarine zones of the York River over an annual cycle. The contribution of large cells (microplankton, >20 μm) to total concentrations of chlorophyll *a* increased downstream during winter, whereas that of small cells (nanoplankton, 3–20 μm; picoplankton, <3 μm) increased downstream during summer. In the freshwater region, the contribution of micro phytoplankton to total concentrations of chlorophyll *a* was significant during warm seasons (spring and summer) but not during colder seasons (winter), whereas the contribution of small-sized cells (especially picoplankton) increased during cold seasons. Temperature, light and high flushing rate appear to control phytoplankton community structure in the freshwater region. In the transitional region, nano-sized cells dominated the phytoplankton population throughout all seasons except during the spring bloom (April) when the chlorophyll *a* concentration of micro phytoplankton increased. Size structure in the transitional region is most likely regulated by light availability. In the mesohaline region, nano- and pico-sized cells dominated the phytoplankton population during the summer bloom, whereas micro-sized cells dominated during the winter bloom. Factors controlling phytoplankton community size structure in the mesohaline zone may be riverine nitrogen input, temperature and/or advective transport from up-river. Based on these results, the spatial and seasonal variations in size structure of phytoplankton observed on the estuarine scale may be determined both by the different preferences for nutrients and by different light requirements of micro-, nano- and picoplankton. The results suggest that analyses of phytoplankton size structure are necessary to better understand controls on phytoplankton dynamics and to better manage water quality in river-dominated, estuarine systems.

## Introduction

One approach to a better understanding of phytoplankton dynamics is to fractionate phytoplankton assemblages into different size classes, as cell size influences both the response of phytoplankton communities to environmental variation (Malone and Chervin, 1979; Takahashi and Bienfang, 1983; Gieskes and Kraay, 1986; Joint and Pomroy, 1986; Oviatt *et al*., 1989; Glibert *et al*., 1992; Armstrong, 1994; Hein *et al*., 1995), and associated impacts on aquatic food web structure and fisheries (Walsh, 1976; Lenz, 1992; Painting *et al*., 1993). Over various time scales, watershed inputs to estuarine systems may change both the quality (size structure) and quantity (biomass) of primary producers. In turn, these changes resulting from environmental disturbance may impact nutrient and dissolved oxygen (DO) distributions, as well as heterotrophic consumers, in the water column. As cell size influences sinking (Michaels and Silver, 1988) and transport rates, it will determine where ungrazed biomass accumulates and undergoes microbial processing by bacteria and protozoa, which, in turn, influences oxygen dynamics (Jonas, 1992) and nutrient remineralization (Caron,

1991). Remineralized nutrients may subsequently support primary production (Kemp and Boynton, 1984).

In past studies, estuarine phytoplankton were usually categorized into two size fractions: netplankton (20–200 μm) and nanoplankton (<20 μm). However, in recent years picoplankton (0.2–2 μm), composed of minute chroococcoid cyanobacteria and eukaryotic phytoplankton, have received attention in estuarine phytoplankton studies (Ray *et al*., 1989; Lacouture *et al*., 1990; Malone *et al*., 1991; Iriarte, 1993).

The EPA (Environmental Protection Agency) Chesapeake Bay Program has monitored chlorophyll *a* (Chl *a*) concentrations as a water quality parameter once or twice per month since mid-1980 in the York River estuary. However, Chl *a* content was not determined for the different size classes. Therefore, to better understand plankton processes in the York River estuary, studies on the size structure dynamics of phytoplankton were undertaken. The principal goals of this study were to: (i) examine temporal and spatial variations in chlorophyll *a* of various size classes of phytoplankton in the York River estuary; (ii) investigate mechanisms controlling size structure dynamics.

## Method

### *Study site and sample collection*

The York River system, a subestuary of the Chesapeake Bay, is composed of three rivers: the York, Pamunkey and Mattaponi (Figure 1). The York River is formed by the confluence of the Pamunkey and Mattaponi rivers at West Point, 48 km from its mouth. The salinity distribution in the York River system is affected by the interactions of fresh water, salt water, tidal energy and wind. Salinity gradients between the surface and bottom layers are influenced by neap and spring tidal cycles, with destratification of the water column occurring at high spring tides and stratification developing during intervening periods (Haas, 1975). Three stations along the axis of the York and Pamunkey Rivers (Figure 1) were sampled over one annual cycle during spring high tides on August 8, 1996, August 15, August 21, September 26, November 11, January 23, 1997, February 20, March 10, April 7, and June 4. One sample (August 8, 1996) was collected at low neap tide. The stations represent the tidal fresh (Station I), river-estuary transition (Station II) and mesohaline zones (Station III) in the York River estuarine system. Samples were collected from 1 m below the surface and 1 m above the bottom using either a water pump or Nanssen bottle. Bottom concentrations of nutrients and Chl *a* were not measured from November 1996 or February 1997 to June 1997 at Station I.

### *Chlorophyll a measurement*

In this study, phytoplankton were grouped into three size classes: micro-size (>20 μm), nano-size (3–20 μm) and pico-size (<3 μm). Phytoplankton were fractionated by filtration through 20 μm Nytex® mesh (1–2 l) and 3 μm PORETICS® polyester membrane filters (1 l) with minimal vacuum (<150 mm Hg). For Chl *a*

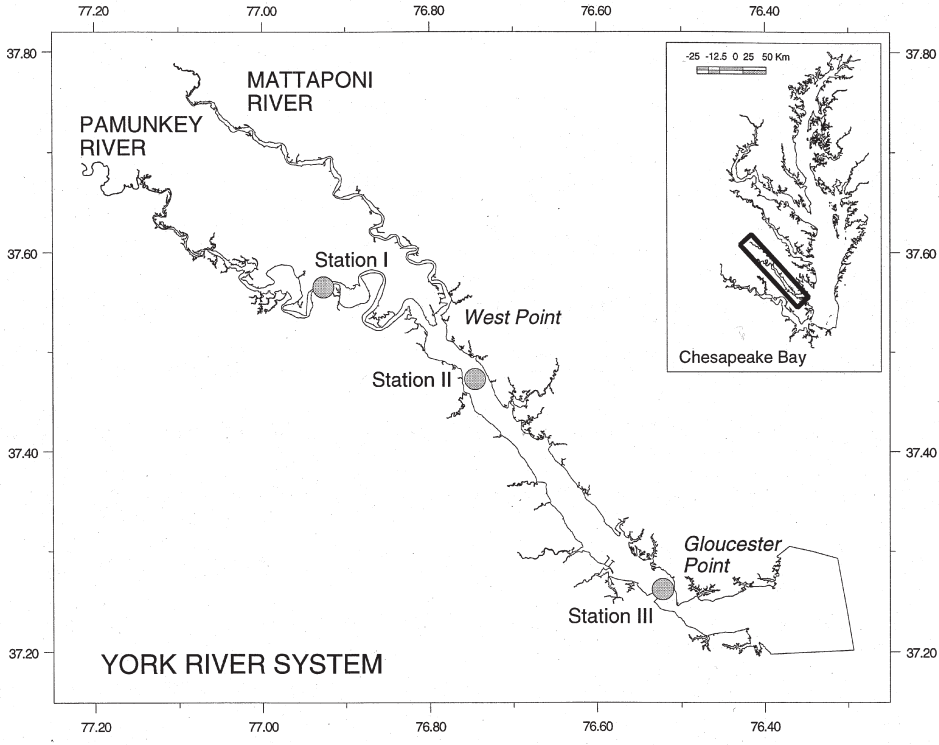


**Fig. 1.** Sampling stations in the tidal freshwater (Station I), transitional (Station II) and mesohaline (Station III) regions of the York River estuary.

determinations, 10 ml of non-fractionated whole water, 20 ml of 20 μm filtrate and 40 ml of 3 μm filtrate were filtered through Whatman® 25 mm GF/F™ glass fiber filters (0.7 μm) under vacuum (<120 mm Hg). Sample filtration was performed in duplicate and immediately following sampling to minimize any potential grazing effects. The filters were placed in dark test tubes pre-filled with 8 ml extraction solution [45% dimethyl sulfoxide (DMSO), 45% acetone, 10% deionized water and 1% diethylamine (DEA) (Webb and Hayward, unpublished)]. After storage for 12 h at room temperature, fluorescence was measured on a Turner Designs® 10-AU fluorometer. Two drops of HCl (2N) were added and the extracts re-read for determination of pheopigments following acidification. Grazers convert Chl *a* to pheopigments, which are released as egested fecal material. The ratio of Chl *a* and pheopigments, determined by the ratios of fluorescence before and after acidification, is an indirect measure of grazing activity [e.g. (Welschmeyer and Lorenzen, 1985)]; the lower the ratio, the higher the grazing rates. Suspended pheopigments can also be produced within phytoplankton cells during senescence as a result of poor growth environments or prolonged exposure to the dark (Yentsch, 1967; Daley and Brown, 1973). Chl *a* in each size fraction was determined by consecutive subtraction of the <3 μm and <20 μm fractions from whole water Chl *a*.

*Measurement of dissolved inorganic nutrients and physical properties*

Water samples (50 ml) for nutrient analyses were filtered (0.45 μm Gelman Supor®) immediately following sampling to minimize microbial transformations and stored refrigerated until analysis. Ammonium was analyzed within 6 h of sampling by the phenolhypochlorite method (Greenberg *et al*., 1992). Samples for nitrite ($NO_2^-$) + nitrate ($NO_3^-$), dissolved silica (Si) and orthophosphate analyses were stored frozen. Nitrite ($NO_2^-$) + nitrate ($NO_3^-$) were measured using an Alpkem® autoanalyzer and orthophosphate ($PO_4^{-3}$) was measured by the molybdate method, as discussed in Parsons *et al*. (Parsons *et al*., 1984). The detection limit of the autoanalyzer is 0.012 μmol $l^{-1}$ for nitrite + nitrate and 0.032 μmol $l^{-1}$ for orthophosphate. Dissolved silica (Si) was measured using a TECHNICON AAII® Continuous Flow Analyzer (Segmented). The procedure for the determination of soluble silicates is based on the reduction of silicomolybdate in acidic solution to molybedenum blue by ascorbic acid (Technicon Industrial Systems, 1973). The detection limit for Si was 0.013 mg $l^{-1}$.

A YSI® Model 33 S-C-T Meter was used to measure *in situ* temperature and salinity during field sampling. A LICOR® PAR Quantum Radiometer was used to measure solar and submarine irradiance at depths of 10, 35, 60, 85 and 110 cm. Light attenuation coefficients were calculated using Beer's Law, $I_z = I_o e^{-kz}$, where $I_z$ is the intensity of light at z, the depth of interest, $I_o$ is the intensity at the surface, and k is the attenuation coefficient of water. Water depth was measured using either a sonar depth meter installed on the boat or a scale marked on the Nanssen bottle's line.

*Other data collection and statistical analysis*

Daily mean solar irradiance data were collected at the Virginia Institute of Marine Science (VIMS), Gloucester Point, Virginia, corresponding to Station III (Figure 1). Monthly mean solar irradiance was calculated from the data downloaded from VIMS data archives. Daily discharge rates near the fall line on the Pamunkey River at Hanover were collected by the U.S. Geological Survey, and monthly means were derived from the data. Linear simple and multiple regression analyses were employed to investigate correlations between phytoplankton size class chlorophyll and the various physical and biological variables reported.

## Results

*River discharge and solar irradiance*

River discharge rates for the period from July 1996 to June 1997 (Figure 2A) displayed a seasonality similar to that in the EPA long-term database (Sin *et al*., 1999); rates were high during winter and spring, and low during summer and fall seasons. Discharge rates were extraordinarily high during fall, especially September, probably due to a storm (Figure 2A). Solar irradiance data collected at Gloucester Point also revealed a seasonal trend, with PAR highest during June and lowest during December (Figure 2B).

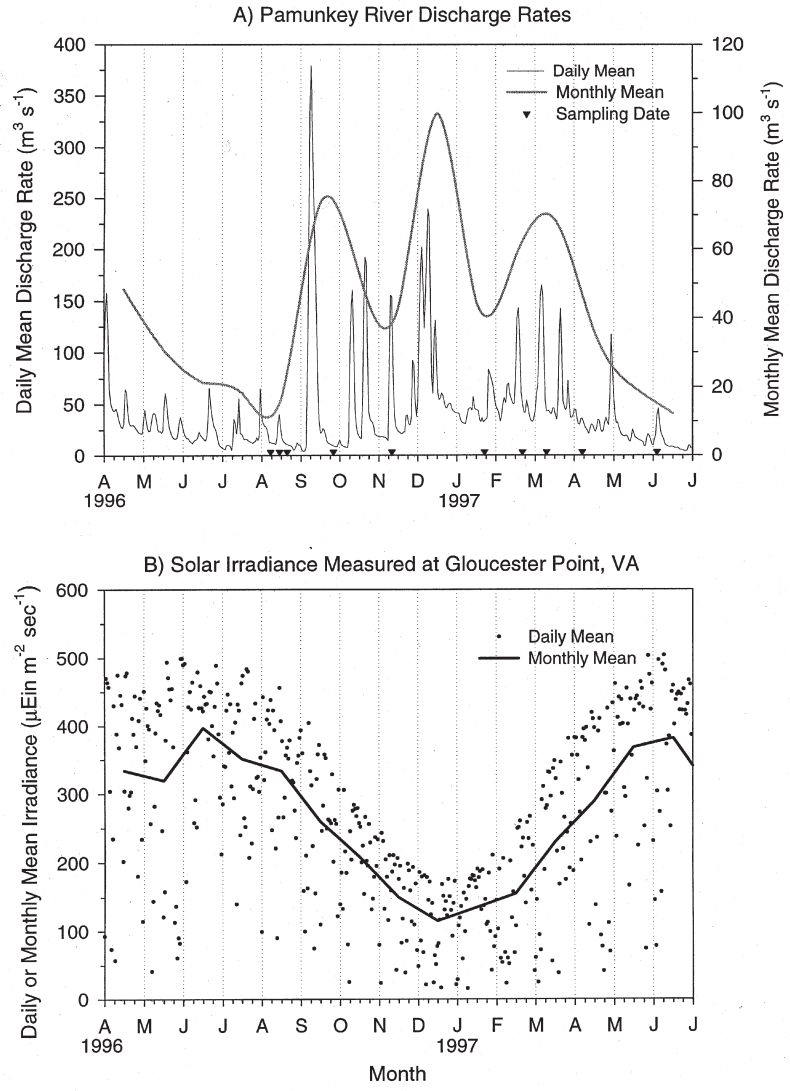


**Fig. 2.** Time series of river discharge rates at fall line of the Pamunkey River (**A**) and surface PAR (µE $m^{-2}$ $s^{-1}$) at Gloucester Point, Virginia (**B**) from April 1996 to June 1997 in the York River estuary.

*Other physical properties; water depth, temperature, salinity and light attenuation*

Water depths at Stations I, II and III were 7.4 ± 0.4, 7.1 ± 0.3 and 16.1 ± 0.5 m, respectively. Water temperatures at all stations were highest during August and lowest during January (Figure 3A, 3B, 3C). Average salinities at Stations II and III for the sampling period were 7.76 ± 1.0 and 15.83 ± 0.53 psu for surface water, and 9.16 ± 0.88 and 18.41 ± 0.64 psu, respectively, for bottom water. Minimum

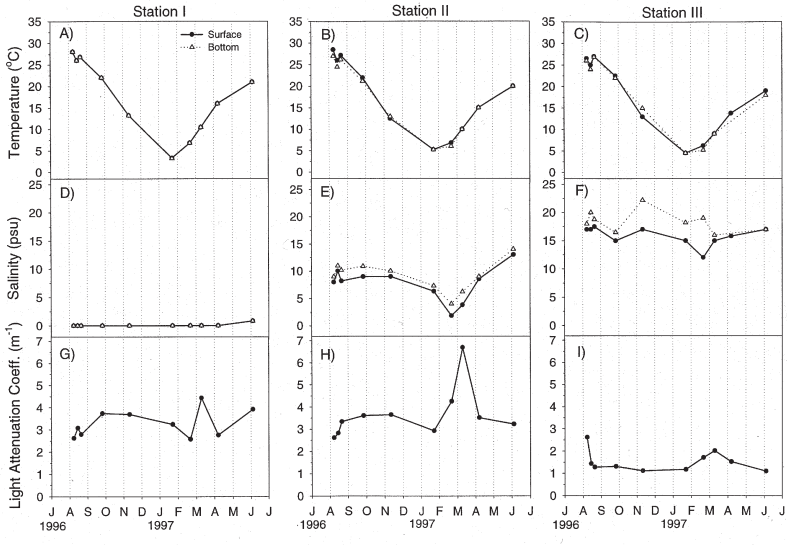


**Fig. 3.** Temperature, salinity and light attenuation coefficient distributions at each station in the York River system.

salinity values were observed at Stations II and III during February and March (Figure 3E, 3F). Average light attenuation coefficients ($K_d$) during the sampling period were 3.28 ± 0.2, 3.66 ± 0.37 and 1.52 ± 0.15 $m^{-1}$ for Stations I, II and III, respectively. $K_d$ was clearly affected by river discharge as it peaked at all stations during March (Figure 3G, 3H, 3I), corresponding to the low salinity values due to high river discharge rates (see Figure 2A).

*Water column dissolved inorganic nutrients*

Figure 4 shows the seasonal variations in concentrations of inorganic nutrients at the study sites. Ammonium concentrations did not vary seasonally at Station I (Figure 4A). They were high during winter and low during summer at Station II (Figure 4B), whereas the reverse pattern was observed at Station III (Figure 4C). Bottom ammonium concentrations at Station III were generally higher than surface concentration throughout the sampling period, especially during summer and fall (Figure 4C).

At Station I, nitrite + nitrate levels were highest during periods of high river discharge, especially February (Figure 4D). Surface nitrite + nitrate concentrations peaked in February at Station II (Figure 4E) and increased at Station III (Figure 4F). Similar seasonal patterns were detected for silicate in surface waters (Figure 4J, 4K, 4L).

There were no clear seasonal variations in orthophosphate concentrations at Station I (Figure 4G). At Stations II and III, orthophosphate concentrations were higher during summer–fall but lower during winter (Figure 4H, 4I). Large

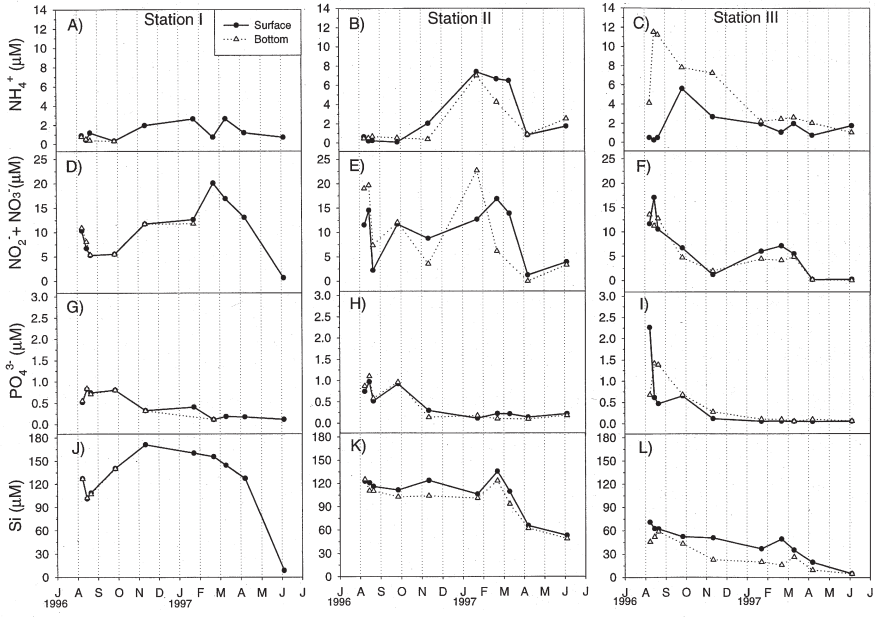


**Fig. 4.** Seasonal distributions of ambient ammonium ($NH_4^+$), nitrite + nitrate ($NO_2^-$ + $NO_3^-$), orthophosphate ($PO_4^{3-}$) and dissolved silicate (Si) at three stations along the axis of the York River system.

differences between surface and bottom water were not observed at Station II. On the other hand, bottom concentrations were generally higher than surface concentrations during August at Station III (Figure 4I).

*Spatial and temporal variations in chlorophyll* a

At Station I, total Chl *a* concentrations in surface water were at a minimum during winter, increased in March and peaked during summer (Figure 5A). This same seasonal Chl *a* signal characterized all phytoplankton size classes at the tidal freshwater station (see Figure 5D, 5G, 5J).

At Station II, surface Chl *a* concentrations were generally higher than at other stations except for the cold season [January, February and March (Figure 5B)]. Chl *a* concentrations of micro phytoplankton significantly increased during the spring bloom (Figure 5E). The seasonal pattern of nano phytoplankton Chl *a* (Figure 5H) was nearly the same as that for total Chl *a* (Figure 5B). Pico phytoplankton Chl *a* was abundant during summer but decreased as temperatures declined (Figure 5K). All size classes had minimum Chl *a* concentrations during the cold season.

Station III showed a clear seasonality, with a small-scale summer bloom and larger-scale winter–spring blooms, when other stations experienced minimum Chl *a* concentrations (Figure 5C). Chl *a* concentrations of micro phytoplankton

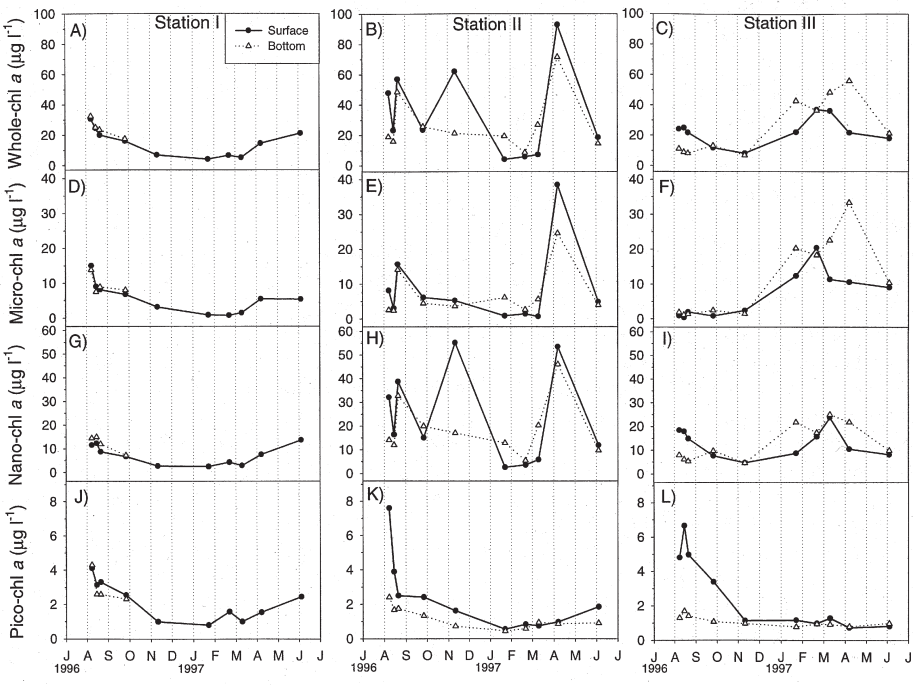


**Fig. 5.** Seasonal distributions of size-fractionated chlorophyll *a* (whole, micro, nano and pico) at three stations along the axis of the York River system.

were highest during winter and lowest during summer in surface water (Figure 5F). Nanophytoplankton Chl *a* had a bimodal pattern with high concentrations during summer and winter–spring (Figure 5I). In contrast to microphytoplankton, picophytoplankton contributed the most to Chl *a* concentrations during summer and the least during winter (Figure 5L). Surface Chl *a* (whole) concentrations were higher than bottom concentrations during summer, especially August, but the opposite was observed during winter–spring (Figure 5C). The peak of Chl *a* (whole) in bottom water coincided with peak bottom Chl *a* concentration of microplankton in April (Figure 5F), and a large surface–bottom difference was observed during this period. The Chl *a* concentrations of micro- and nanophytoplankton were relatively low during summer in bottom water.

In the surface water at Station I, the contribution of large cells (microphytoplankton) to total Chl *a* was high during the warm season, whereas the contribution of small cells (nano-, picophytoplankton) increased rapidly during the cold period (Figure 6A). At Station II, nanophytoplankton Chl *a* dominated the Chl *a* pool throughout the sampling period (Figure 6B), although the contribution from large cells increased rapidly during the spring bloom. Based on Chl *a* measurement at Station III, small cells (nano-, picophytoplankton) dominated the mesohaline phytoplankton community during the warm season, whereas large cells dominated the community during the winter bloom (Figure 6C). Shifts

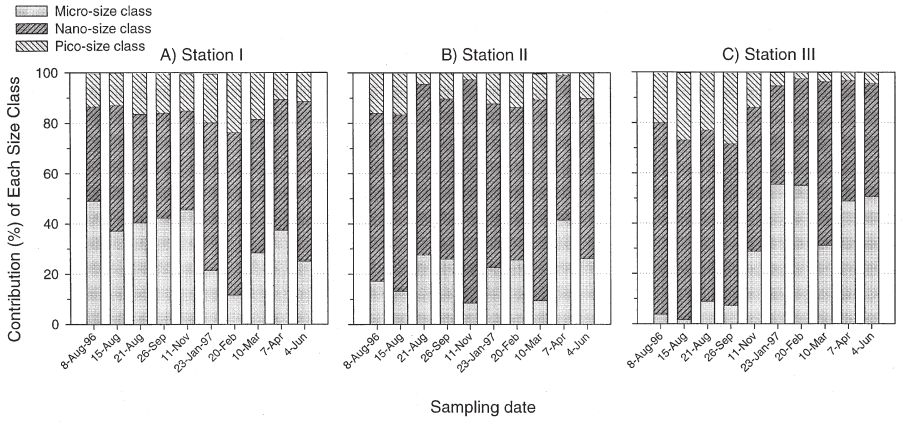


**Fig. 6.** Percentage contributions of three size classes (micro, nano and pico) to the total chlorophyll *a* in the surface water of the study sites of the York River estuary.

in size structure at Station III were initiated in the fall as river discharge rates increased.

*Simple linear and multiple regression analysis*

Table I shows results ($r^2$) of linear regression analyses of relationships between the Chl *a* concentrations of various phytoplankton size classes and various physical and biological properties of the York River estuary, specifically river discharge rates, Chl:Pheo ratio, PAR and water temperature. At Station I, river discharge rates (Q, $m^3 s^{-1}$) were significantly ($\alpha = 0.05$) and negatively correlated with Chl *a* concentrations in unfractionated water. The relationship was similar for the nano-size class ($\alpha = 0.05$) and for micro- and pico-size class ($\alpha = 0.1$). Chl:Pheo ratios were not correlated with any size class Chl *a* at Station I (Table I). PAR and temperature were significantly positively correlated with chlorophyll *a* concentrations of all size classes except the nano-size class for PAR ($\alpha = 0.05$). Multiple regression analysis indicated that river discharge rates, PAR and temperature were responsible for 92% (whole), 87% (micro-size class), 80% (nano-size class) and 89% (pico-size class) of the variation in size class structure at Station I.

At the river estuary transition Station (Station II), river discharge was not correlated with Chl *a* concentrations (Table I); however, Chl:Pheo ratios were significantly and positively correlated with the total Chl *a* pool (whole) ($r^2 = 0.46$; $P < 0.05$) and that of the nano-size class ($r^2 = 0.74$; $P < 0.05$). PAR and temperature were significantly correlated only with Chl *a* concentrations of the pico-size class ($r^2 = 0.73$; $P < 0.05$). Based on multiple regression analysis, PAR and temperature were responsible for 75% of the variation in Chl *a* concentrations of the pico-size class.

**Table I.** Results ($r^2$) of linear regression analysis of surface chlorophyll *a* (μg $l^{-1}$) or percentage contribution by each size class (%) versus river discharge rates (Q, $m^3 s^{-1}$), chlorophyll:pheophytin ratio (Chl:Pheo), PAR at 1 m water depth (PAR μEin $m^{-2} s^{-1}$) and temperature (T, °C) during the sampling period. $r^2$ Values less than 0.1 were omitted and denoted by '–'. Negative value represents negative relationship

| Size class | Station I | | | | Station II | | | | Station III | | | |
|---|---|---|---|---|---|---|---|---|---|---|---|---|
| | Q | Chl:Pheo | PAR | T | Q | Chl:Pheo | PAR | T | Q† | Chl:Pheo | PAR | T |
| Whole | –0.52** | – | 0.54** | 0.86** | 0.12 | 0.46** | – | 0.12 | – | – | –0.19 | 0.12 |
| Micro | –0.36* | –0.15 | 0.58** | 0.81** | – | – | – | – | 0.58** | 0.19 | – | –0.69** |
| Nano | –0.59** | – | 0.35* | 0.68** | 0.10 | 0.74** | – | 0.10 | – | – | 0.14 | – |
| Pico | –0.37* | – | 0.58** | 0.84** | 0.26 | 0.28 | 0.73** | 0.61** | –0.48** | 0.16 | – | 0.66** |

Whole, Micro, Nano, and Pico: total, micro-sized, nano-sized and pico-sized chlorophyll *a*.
†One month-lag time considered.
*$P < 0.1$; **$P < 0.05$.

In the mesohaline zone (Station III), river discharge rates were significantly correlated with Chl *a* concentrations of the micro-size class ($r^2 = 0.58$; $P < 0.05$), whereas temperature was significantly correlated with Chl *a* concentrations of the pico-size class ($r^2 = 0.66$; $P < 0.05$). The negative relationship observed between temperature and the Chl *a* concentration of the micro-size class is likely due to autocorrelation between temperature and river discharge rate. Similarly, the negative relationships between river discharge rates and pico-sized Chl *a* is also likely due to autocorrelation between temperature and river discharge, or to slower growth rates of small cells compared with large cells at high supply rates of nutrients. Based on multiple regression analysis, 69% of the variation in Chl *a* concentrations of the pico-size class was explained by river discharge and temperature. In bottom water, strong positive relationships (data not shown) were observed between river discharge rates and Chl *a* concentrations of unfractionated ($r^2 = 0.95$), micro-size ($r^2 = 0.97$) and nano-size phytoplankton ($r^2 = 0.83$).

## Discussion

The tidal freshwater station (Station I) was thought to be enriched with riverine N and Si input from riverine run-off throughout the year; however, concentrations of nitrite + nitrate were lower than that in the mesohaline zone during summer (see Figure 4D, 4F), most likely due to high uptake by large phytoplankton which reportedly dominate when the supply of nitrate ('new' nitrogen) is high (Eppley and Peterson, 1979; Malone, 1980a,b; Probyn, 1985). On an annual basis, temperature and Chl *a* concentrations for all size classes of phytoplankton were significantly and positively correlated. Although we recognize that this relationship may be confounded by autocorrelation between light and temperature, we observed high chlorophyll *a* in June at a time when temperatures were high and light attenuation in the water column was also high (Figure 3A, 3G and 5A). During early summer, we suggest that rising temperatures were responsible for increased phytoplankton growth and nutrient uptake at Station I. The effects of temperature on the uptake of N and maximum algal growth rates have also been observed by Eppley (Eppley, 1972) and Carpenter and Dunham (Carpenter and Dunham, 1985). Accumulation of phytoplankton Chl *a* biomass may be limited by high flushing rates in the tidal freshwater region during winter, as Chl *a* concentrations were generally inversely correlated with river discharge rate (Table I). Previous studies by Sin *et al.* (Sin *et al.*, 1999) demonstrated that decreased phytoplankton Chl *a* biomass in the freshwater portions of the river resulted from the long mean doubling times of phytoplankton relative to residual velocities calculated by a hydrodynamic model. We observed that the contribution of pico-sized phytoplankton to total Chl *a* concentrations was negatively correlated with total Chl *a* ($r^2 = 0.41$, $P < 0.05$). Chisholm similarly observed that the percentage of small cells in the phytoplankton community increased as total Chl *a* decreased (Chisholm, 1992).

Controls on phytoplankton dynamics in the river estuary transition zone (Station II) are more complex. The river estuary transition region is the site of the turbidity maximum, whose location and degree of mixing are controlled by

the river discharge rate (Hansen and Rattray, 1965). Based on the measured light attenuation coefficients, the turbidity maximum developed during February and March (Figure 3H). The Chl *a* minima observed during winter at Station II corresponded with the peak light attenuation coefficient (see Figure 5B). Thus, phytoplankton growth in this river estuary transitional zone was likely limited by light during the cold season when river discharge rates were high. The low Chl:Pheo ratios observed during the cold season (data not shown) may have resulted from autolysis of phytoplankton under light-limited conditions, or grazing. Pheopigments, which are released as egested fecal material by grazers, have been used as an indicator of herbivorous grazing [e.g. (Shuman and Lorenzen, 1975; Welschmeyer and Lorenzen, 1985)]. Suspended pheopigments can also be produced within phytoplankton cells during senescence caused by poor growth environments or prolonged exposure to the dark (Yentsch, 1967; Daley and Brown, 1973). Thus, it is difficult to distinguish the relative importance of grazing versus light limitation in regulating the phytoplankton community in the river estuary transition zone. However, it has been suggested that phytoplankton dynamics in the York River are regulated primarily by resource limitation (bottom-up control) rather than zooplankton grazing (top-down control) in the estuary (Sin *et al*., 1999). In this context, the phytoplankton community is more likely controlled by light limitation than zooplankton grazing in this region. Chl *a* concentrations of whole and nano-sized classes were significantly correlated with Chl:Pheo ratios (Table I).

As discussed in Sin *et al*. (1999), nitrogen may limit phytoplankton growth in the mesohaline zone during spring–summer. The Chl *a* concentrations of small cells (pico- and nano-size classes) which dominated during summer were most closely correlated with temperature (Table I). During late summer and early fall, high temperatures increase remineralization of organic nitrogen and phosphate in sediments, thereby releasing ammonium and orthophosphate which accumulate in bottom water (Fig. 4C, 4I) under stratified conditions and are supplied to surface water through spring–tidal destratification (tidal mixing) in the lower York River (Webb and D'Elia, 1980). The regenerated ammonium and orthophosphate can stimulate growth of small phytoplankton in surface water. Regenerated ammonium was considered to be the primary nutrient source for picoplankton and nanoplankton production in the southern Benguela upwelling system during winter (Probyn, 1985). In this study, nitrite + nitrate concentrations were relatively high in surface water during summer, especially August (Figure 5C), but ammonium concentrations were low (Figure 5F), suggesting that small phytoplankton may prefer ammonium to nitrite + nitrate.

The strong correlation between Chl *a* derived from microphytoplankton and river discharge rates at Station III suggests that river discharge rates determine the location and magnitude of winter–spring blooms which, in turn, sink and contribute to high Chl *a* concentrations in bottom water. Based on results of regression analyses (Table I), and as reported by others (Eppley and Peterson, 1979; Malone, 1980a,b; Probyn, 1985), large phytoplankton cells (micro-sized) dominate in areas with high supply rates of new nitrogen, as observed during winter–spring when river discharge rates are highest. However, it is difficult to

distinguish the relative importance of *in situ* production supported by riverine N input versus advective transport of microphytoplankton from the upper river as a principal source for winter–spring blooms of microphytoplankton. These results demonstrate that analyses of size structure phytoplankton dynamics are necessary to understand the response of the total phytoplankton population to environmental change in estuarine systems.

With respect to spatial variations, it has been observed (Malone, 1980b) that small cells tend to be more abundant as one moves down the estuary. Iriarte found that Chl *a* concentrations in the >1 μm fraction were highest midway down the estuary and decreased both in landward and seaward directions (Iriarte, 1993). In contrast, Chl *a* concentrations in the small-sized (0.2–1 μm) fraction were highest at the seaward end of the estuary. A similar trend was observed for small size classes (0.2–3 μm) in a study by Lacouture *et al*. (Lacouture *et al*., 1990); observations made here are similar to those of Lacouture *et al*. in that contributions of small cells (nano-, pico-sized) to total Chl *a* concentrations increased down-estuary during summer and the dominance of large cells increased down-estuary during winter (Figure 6).

The factors which appear to regulate the relative abundance of various size fractions of phytoplankton along the estuarine gradient, and with depth in the water column, are availability of regenerated ammonium relative to new nitrogen and light availability. Whereas small cells are favored by the relatively higher ammonium concentrations and greater light availability occurring downstream, larger cells are favored by the relatively higher nitrate concentrations and lower light availability upstream [c.f. (Laws, 1975)]. The position of phytoplankton in the water column is also determined by sinking and vertical migration rates. For example, the greater abundance of dinoflagellates in surface waters during winter–spring may, in part, be determined by their ability to more efficiently undergo diel vertical migrations (Blasco, 1978; Villarino *et al*., 1995).

## Conclusions

Phytoplankton growth in the tidal freshwater zone is most likely limited by high flushing rates and regulated by light availability and temperature-dependent metabolism. The large contribution of microplankton-derived Chl *a* to the Chl *a* pool during late summer and fall is thought to be due to the greater availability of nitrite + nitrate upstream compared with downstream stations in the York River estuary. In the river estuary transition zone, phytoplankton production is most likely limited by light availability, as this region experiences a turbidity maximum during the winter–spring period. Nanoplankton, which dominate the phytoplankton community in the river estuary transition zone throughout the year, are most likely regulated by light availability. Growth of large cells in this zone is dependent on nitrite + nitrate input, but only when light is not limiting. In the mesohaline zone, total Chl *a* concentration follows a bimodal seasonal distribution with both summer and winter blooms. During summer, small cells (picoplankton and nanoplankton) dominate while during winter, large cells (microplankton) dominate. This seasonal shift in size structure is thought to be

due to the different preferences of phytoplankton size classes for 'new' (nitrite + nitrate) versus 'old' (ammonium) nutrients in the water column. We conclude from these studies that spatial and seasonal variations in size structure of phytoplankton observed on the estuarine scale are determined both by the different preferences of micro-, nano- and picoplankton for nutrients, and by their different light requirements coupled to river discharge. These results further indicate that phytoplankton size structure in the York river estuary may be regulated primarily by resource limitation (bottom-up control) rather than zooplankton grazing (top-down control). Consequently, the present study supports the conclusions established from the EPA long-term data analyses on phytoplankton and nutrient dynamics (Sin *et al*., 1999), and further demonstrates that analyses of size structure phytoplankton dynamics are necessary to better understand phytoplankton dynamics, including the response of the total phytoplankton population to environmental change in estuarine systems.

## Acknowledgements

We are indebted to Dr L.W.Haas, Dr H.W.Paerl and Dr H.W.Ducklow for their valuable discussions and insights. This research was supported in part by grants to R.L.W. from the U.S. EPA Chesapeake Bay Program (CB993267–02–1) and AMOCO, Inc., Yorktown, Virginia. This is contribution number 2309 from the Virginia Institute of Marine Science, School of Marine Science of the College of William and Mary, VA (USA).

## References

Armstrong,R.A. (1994) Grazing limitation and nutrient limitation in marine ecosystems: Steady state solutions of an ecosystem model with multiple food chains. *Limnol. Oceanogr*., **39**, 597–608.

Blasco,D. (1978) Observations on the diel migration of marine dinoflagellates off the Baja California coast. *Mar. Biol.*, **46**, 41–47.

Caron,D.A. (1991) Evolving role of protozoa in aquatic nutrient cycles. In Ried,P.C., Turley,C.M. and Burkill,P.H. (eds), *Protozoa and their Role in Marine Processes*. NATO ASI, Springer-Verlag, Berlin, Heidelberg, **G 25**, pp. 387–415 (5.3).

Carpenter,E.J. and Dunham,S. (1985) Nitrogenous nutrient uptake, primary production, and species composition of phytoplankton in the Carmans River estuary, Long Island, New York. *Limnol. Oceanogr*., **30**, 513–526.

Chisholm,S.W. (1992) Phytoplankton size. In Falkowski,P.G. and Woodhead,A.D. (eds), *Primary Productivity and Biogeochemical Cycles in the Sea*. Plenum Press, New York, pp. 213–237.

Daley,R.J. and Brown,S.R. (1973) Experimental characterization of lacustrine chlorophyll diagenesis. 1. Physiological and environmental effects. *Arch. Hydrobiol*., **72**, 277–304.

Eppley,R.W. (1972) Temperature and phytoplankton growth in the sea. *Fish. Bull*., **70**, 1063–1085.

Eppley,R.W. and Peterson,B.J. (1979) Particulate organic matter flux and planktonic new production in the deep ocean. *Nature*, **282**, 677.

Gieskes,W.W. and Kraay,G.W. (1986) Floristic and physiological differences between shallow and the deep nanophytoplankton communities in the euphotic zone of the tropical Atlantic ocean revealed by HPLC analysis of pigments. *Nature*, **91**, 567–576.

Glibert,P.M., Miller,C.A., Garside,C., Roman,M.R. and McManus,G.B. (1992) $NH_4^+$ regeneration and grazing: interdependent processes in size-fractionated $^{15}NH_4^+$ experiments. *Mar. Ecol. Prog. Ser*., **82**, 65–74.

Greenberg,A.E., Clesceri,L.S. and Eaton,A.D. (1992) *Standard Methods for the Examination of Water and Wastewater,* Vol. 18. American Public Health Association, Washington D.C.

Haas,L.W. (1975) Plankton dynamics in a temperate estuary with observations on variable

hydrographic conditions. Doctoral dissertation, School of Marine Science, College of William and Mary, Gloucester Point, Virginia.
Hansen,D.V. and Rattray Jr, M., (1965) Gravitational circulation in straits and estuaries. *J. Marine Res.*, **23**, 104–122.
Hein,M., Pedersen,M.F. and Sand-Jensen,K. (1995) Size-dependent nitrogen uptake in micro- and macroalgae. *Mar. Ecol. Prog. Ser.*, **118**, 247–253.
Iriarte,A. (1993) Size-fractionated chlorophyll *a* biomass and picophytoplankton cell density along a longitudinal axis of a temperate estuary (Southampton Water). *J. Plankton Res.*, **15**, 485–500.
Joint,I.R. and Pomroy,A.G. (1986) Photosynthetic characteristics of nanoplankton and picoplankton from the surface mixed layer. *Mar. Biol.*, **92**, 465–474.
Jonas,R. (1992) Microbial processes, organic matter and oxygen demand in the water column. In Smith,D.E., Leffler,M. and Mackiernan,G. (eds), *Oxygen Dynamics in the Chesapeake Bay*. Maryland Sea Grant College, College Park, pp. 113–148.
Kemp,W.M. and Boynton,W.R. (1984) Spatial and temporal coupling of nutrient inputs to estuarine primary production: the role of particulate transport and decomposition. *Bull. Mar. Sci.*, **35**, 522–535.
Lacouture,R.V., Wagoner,B.B., Nealley,E. and Seller,K.G. (1990) Dynamics of the microbial food web in the Patuxent River: autotrophic picoplankton. In Mihursky,J.A. and Chaney,A. (eds), *New Perspectives in the Chesapeake System: A Research and Management Partnership*. Chesapeake Research Consortium Publication No. 137, pp. 297–307.
Laws,E.A. (1975) The importance of respiration losses in controlling the size distribution of marine phytoplankton. *Ecology*, **56**, 419–426.
Lenz,J. (1992) Microbial loop, microbial food web and classical food chain: Their significance in pelagic marine ecosystems. *Arch. Hydrobiol. Beih.*, **37**, 265–279.
Malone,T.C. (1980a) Agal size. In Morris,I. (ed.), *The Physiological Ecology of Phytoplankton.* Blackwell Scientific Publishers, Oxford, UK, pp. 433–463.
Malone,T.C. (1980b) Size-fractionated primary productivity of marine phytoplankton. In Falkowski,P.G. (ed.), *Primary Productivity in the Sea*. Plenum, New York/London, Vol. 31, pp. 161–178.
Malone,T.C. and Chervin,M.B. (1979) The production and fate of phytoplankton size fractions in the plume of Hudson River, New York Bight. *Limnol. Oceanogr.*, **24**, 683–696.
Malone,T.C, Ducklow,H.W., Peele,E.R. and Pike,S.E. (1991) Picoplankton carbon flux in Chesapeake Bay. *Mar. Ecol. Prog. Ser.*, **78**, 11–22.
Michaels,A.E. and Silver,M.W. (1988) Primary production, sinking fluxes and the microbial food web. *Deep-Sea Res.*, **35**, 473–490.
Oviatt,C., Lane,P., French,F. III and Donaghay,P. (1989) Phytoplankton species and abundance in response to eutrophication in coastal marine mesocosms. *J. Plankton Res.*, **11**, 1223–1244.
Painting,S.J., Moloney,C.L. and Lucas,M.I. (1993) Simulation and field measurements of phytoplankton-bacteria-zooplankton interactions in the southern Benguela upwelling region. *Mar. Ecol. Prog. Ser.*, **100**, 55–69.
Parsons,T.R., Maita,Y. and Lalli,C.M. (1984) *A Manual of Chemical and Biological Methods for Seawater Analysis*. Pergamon Press, New York, pp. 22–25.
Probyn,T.A. (1985) Nitrogen uptake by size-fractionated phytoplankton populations in the southern Benguela upwelling system. *Mar. Ecol. Prog. Ser.*, **22**, 249–258.
Ray,T.R., Haas,L.W. and Sieracki,M.E. (1989) Autotrophic picoplankton dynamics in a Chesapeake Bay sub-estuary. *Mar. Ecol. Prog. Ser.*, **52**, 273–285.
Shuman,F.R. and Lorenzen,C.M. (1975) Quantitative degradation of chlorophyll by a marine herbivore. *Limnol. Oceanogr.*, **20**, 580–586.
Sin,Y., Wetzel,R.L. and Anderson,I.C. (1999) Spatial and temporal characteristics of nutrient and phytoplankton dynamics in the York River estuary, Virginia: Analyses of long term data. *Estuaries*, **22**, 260–275.
Takahashi,M. and Bienfang,P.K. (1983) Size structure of phytoplankton biomass and photosynthesis in subtropical Hawaiian waters. *Mar. Biol.*, **76**, 203–211.
Technicon Industrial Systems (1973) *Technicon AutoAnalyzer II Industrial Method No. 186–72W, Silicates in Water and Seawater*.
Villarino,M.L., Figueiras,F.G., Jones,K.J., Alvarez-Delgado,X.A., Richard,J. and Edwards,A. (1995) Evidence of *in situ* diel vertical migration of a red-tide microplankton species in Ria de Vigo (NW Spain). *Mar. Biol.*, **23**, 607–617.
Walsh,J.J. (1976) Herbivory as a factor in patterns of nutrient utilization in the sea. *Limnol. Oceanogr.*, **21**, 1–13.
Webb,K.L. and D'Elia,C.F. (1980) Nutrient and oxygen redistribution during a spring neap tidal cycle in a temperate estuary. *Science*, **207**, 983–985.

Welschmeyer,N.A. and Lorenzen,C.J. (1985) Chlorophyll budgets: Zooplankton grazing and phytoplankton growth in a temperate fjord and the Central Pacific Gyres. *Limnol. Oceanogr.*, **30**, 1–21.
Yentsch,C.S. (1967) The measurement of chloroplastic pigments—thirty years of progress? In Golterman,H.C. and Clymo,R.S. (eds), *Chemical Environment in the Aquatic Habitat*. North-Holland, Amsterdam, pp. 225–270.

*Received on October 18, 1999; accepted on May 15, 2000*